UNIVERSITY OF OKLAHOMA

GRADUATE COLLEGE

THE IMPACT OF TITANIUM DIOXIDE NANOPARTICLES ON THE SPOILAGE BACTERIAL GROWTH ON SPINACH LEAVES

A THESIS

SUBMITTED TO THE GRADUATE FACULTY

in partial fulfillment of the requirements for the

Degree of

MASTER OF SCIENCE

By

NOUR ALFAILAKAWI
Norman, Oklahoma
2023

THE IMPACT OF TITANIUM DIOXIDE NANOPARTICLES ON THE SPOILAGE BACTERIAL GROWTH ON SPINACH LEAVES

A THESIS APPROVED FOR THE
SCHOOL OF CIVIL ENGINEERING AND ENVIRONMENTAL SCIENCE

BY THE COMMITTEE CONSISTING OF

Dr. Keith Strevett

Dr. Tohren Kibbey

Dr. Jason Vogel

DEDICATION

This thesis is dedicated to my parents, Nahedah and Khaled Alfailakawi, whose support and encouragement has been unfaltering and enthusiastic, even when it was not easy to give it. I also dedicate this work to my sisters Dalal, Mariam, and Fay, who have never left my side.

ACKNOWLEDGEMENTS

This research study owes a lot of gratitude to my advisor, Dr. Strevett, who always provides support, courage, and invaluable advice. I would also like to acknowledge and give my warmest thanks to Dr. Kibbey, who never fails to help improve this work. Many thanks go to Dr. Vogel for his valuable feedback.

TABLE OF CONTENTS

LIST OF TABLES

LIST OF FIGURES

ABSTRACT

Nanoparticles are increasingly being considered for various agricultural applications, ranging from nano-based fertilizers to nano-pesticides that can easily attach to the produce. This work aspires to isolate spoilage bacteria from spinach leaves, determine the surface electrodynamic energies of bacteria isolates, evaluate the impact of nanoparticles on bacterial attachment from leafy vegetables, and determine the changes in Lifshitz-van der Waals and Lewis Acid/Base interfacial forces of bacteria in the surface with and without the presence of nanoparticles. It was hypothesized that titanium dioxide reduces the growth of spoilage bacteria on spinach leaves. The methods were divided into six sections: bacterial growth, isolating bacterial consortiums, contact angle measurements, xDLVO model, bacterial growth with the presence of titanium dioxide, and statistical analysis. Spinach spoilage took 35 days to form; LB media (Lysogeny broth) was used then for bacterial growth as the most recognized bacteria found was likely to be *Erwinia* species.

It was found that the addition of high titanium dioxide concentrations resulted in a decreased number of colony-forming units. Still, low titanium dioxide concentrations showed no statistical difference from bare spinach leaves. The Gibbs free energies of attachment for both Lifshitz-van der Waals and Lewis acid-base interactions were calculated to be negative for *Erwinia* with spinach leaves but positive for Erwinia with titanium dioxide. Because negative free energies correspond to a favorable interfacial thermodynamic interaction, and positive free energies correspond to an unfavorable interaction, this difference may partially explain the different observed spoilage behaviors in the absence and presence of titanium dioxide.

CHAPTER 1. INTRODUCTION

Nanoparticles are usually defined as particles between 1 and 100 nanometers in diameter. These particles are increasingly being considered for various agricultural applications, ranging from nano-based fertilizers to nano-pesticides that can easily attach to the produce. Nanoparticles can enhance crop growth by motivating the activity of enzymes, improving photosynthesis, enhancing nutrient absorption, and improving crop yield and quality (Chaudhary & Singh, 2020). Although nanoparticles have many potential benefits in agriculture, they also may have risks for human and ecological health. Local lung inflammation is the primary health risk associated with nanoparticles (Pestovsky & Martinez-Antonio, 2017).

Most microorganisms that are observed on produce surfaces are soil inhabitants. They are members of a vast and diverse community of microbes that collectively are responsible for maintaining a dynamic ecological balance within agriculture systems. Spoilage microorganisms can be introduced to crops from contaminated seeds during crop growth, harvesting, postharvest handling, or storage and distribution. Spoilage microorganisms exploit the host using extracellular lytic enzymes that degrade their polymers to release water and the plant's other intracellular constituents to use as nutrients for their growth (Barth et al., 2009). Lytic enzymes are enzymes produced by bacteria viruses to digest the bacterial cell wall. It has been reported that the most common bacteria present in spinach leaves are the *Erwinia* species (sp.). *Erwinia sp.* is one of the *Pseudomonas* genera and is a highly effective microbe that could soft rot over a broad host range of vegetables and fruits (Jackson et al., 2013).

This work aimed to isolate spoilage bacteria from spinach leaves, determine the surface thermodynamic energies of bacterial isolates, evaluate the impact of nanoparticles on bacterial attachment from leafy vegetables, and determine the changes in Lifshitz-van der Waals and Lewis Acid/Base interfacial forces of bacteria in the surface with and without the presence of nanoparticles. Previous work found that adding titanium dioxide reduced bacterial populations in the spoil and rhizosphere of lettuce plants (Kibbey & Strevett, 2019). Evidence from that work suggested that the titanium dioxide was likely inhibiting the attachment or function of bacteria in the rhizosphere. It was hypothesized in this work that titanium dioxide similarly reduces the growth of spoilage bacteria on spinach leaves.

This work investigated the Lifshitz-van der Waals and Lewis acid-base attachment energies to gain insight into how nanoparticles might impact bacterial attachment and colonization. The overall work of adhesion combines Lifshitz-van der Waals, Lewis acid-base, and electrostatic interactions (Chen & Strevett, 2001). Lifshitz-van der Waals was the first proposed concept of an attractive general interaction between atoms to account for specific properties of nonideal gases and liquids (Van Oss et al., 1988). Lifshitz-van der Waals interactions occur when molecules come near enough that their external electron pair clouds hardly touch. Lewis acid-base interaction occurs when bases donate pairs of electrons, and acids accept pairs of electrons.

This study's research question is: What is the impact of titanium dioxide on the bacterial growth cultivated from spoiled spinach? The hypothesis is that titanium dioxide reduces the growth of spoilage bacteria on spinach leaves. This study aims to: (i) isolate spoilage bacteria from spinach leaves; (ii) determine the surface

electrodynamic energies of bacteria isolates; (iii) evaluate the impact of nanoparticles on bacterial attachment from leafy vegetables; (iv) determine the changes in Lifshitz-van der Waals interfacial forces of bacteria to the surface with and without the presence of nanoparticles and bacteria; and (vi) determine the changes in Lewis Acid/Base interfacial forces of bacteria to the surface with and without the presence of nanoparticles and bacteria.

CHAPTER 2. LITERATURE REVIEW

2.1 Produce

Spinach leaf is considered a cool-season vegetable crop as the seeds can grow at a temperature range between 35º to 85ºF (Koike et al., 2011). A freezing climate can cause harm to the tiny seedlings and young plants, although the more developed plants can endure a freezing climate for weeks. Sandy loam soils are preferred for spinach production as it is direct-seeded and sensitive to saturated conditions, which participate in soilborne infections and rotting of the roots, crown, and lower leaves. Koike et al. (2011) stated that the damage from microorganisms could also spoil spinach; they require water and nutrients to grow. Spinach production mainly needs 2 to 4 inches of water to be sprayed to moisten the soil. The amount of irrigation may differ depending on local rainfall. The crops mostly require two to three irrigations between seeding and rise. Intense irrigation may be required during spring and summer with a brief sprayer every two days since the moisture will most likely evaporate (Koike et al., 2011).

Spinach is moderately fertilized, with the fertilizer rate depending on the type of spinach production, soil type, recent copping history, and soil test results (Kioke et al., 2011). Depending on the soil test results for extractable bicarbonate phosphorus, phosphorus fertilizers may be applied to improve spinach growth. While potassium fertilizers cause no environmental harm, it is being applied routinely by many farmers since it is suitable to preserve soil richness for fresh market spinach. On the other hand, nitrogen fertilizers have a significant risk of NO_3-N leaching past the root zone by the downpours season. However, a small amount is applied as it is adequate for new production.

A study was made on the effect of growth temperature and temperature shifts on spinach leaf morphology and photosynthesis. Boese and Hunter (1990) mentioned that spinach was frequently used in cold acclimation and freezing tolerance studies since it is a cold-tolerant plant. Cold-tolerant plants are the plants that can survive a frost below freezing temperature. Boese and Hunter (1990) objectives included the effects of leaf development at low temperatures and the effect of a temperature shift on leaf anatomy and cold tolerance in spinach. They also compared the presence of cold-tolerance spinach to growth and development at low temperatures and a temperature shift for cold-tolerant rye. The results indicated that the growth and development at low temperatures were not strictly comparable with the effects of an abrupt temperature shift (Boese & Hunter, 1990). They also found a species-dependent reduction in photosynthetic efficiency by an abrupt temperature.

Naznin et al. (2019) studied adding blue light with red LEDs to enhance spinach leaves' growth characteristics and pigment content in a closed production system. They stated that spinach is a rich source of nutrients, making it a popular plant with consumption steadily increasing globally. Their results indicated that the red and blue LEDs did not significantly influence the plant height of spinach leaves (Naznin et al., 2019). However, Naznin et al. (2019) did find that a significantly high leaf number, high fresh and dry mass, and high carotenoid (i. e. tetraterpenoids) accumulation has been observed by using blue and red LEDs to enhance the growth of spinach.

2.2 Nanoparticles

Nanoparticles are particles between 1 and 100 nanometers in diameter. The main potential applications of nanoparticles in agriculture are fertilizers or plant growth stimulants, nano pesticides, carriers of conventional pesticides, and antibacterial agents (Pestovsky & Martinez-Antonio, 2017). A study was made by Abdulhameed et al. (2021) on the influence of cerium oxide nanoparticles and nitrogen, phosphorus, and potassium (NPK) nano fertilizers on the growth and yield of the cabbage plant. The goal was to find a system to increase production so it would be enough to feed the population growth. The research object was to investigate the progress of cabbage growth and yield by fertilizing it with chemical NPK fertilizers and nano NPK fertilizers and enhancing it with CeO_2 NPs during one season of implantation. The work involved five sample transactions with three replicates containing 45 plants. The fertilization process started after one week of planting, adding fertilizer every 21 days to each plant. While the CeO_2NPs were added to each plant after one month of planting, the crops were harvested after fertilization during one agricultural season. The study found that plants treated with nano NPK fertilizers had the highest average head circumference, average head weight, and total plant yield. Abdulhameed et al. (2021) stated that nano fertilization backed with nanoparticles supplied the plants' need for essential nutrients with high values according to the vegetative characteristics compared with the chemical fertilization and control plants.

In separate work, the effects of nanoparticles on soil and rhizosphere bacteria and plant growth in lettuce seedlings were studied (Strevett & Kibbey, 2019). The rhizosphere is defined by MucNear (2013) as the thin layer of the soil attached to the

plant roots in the unsaturated zone of the subsurface. It is the area around a plant root inhabited by a unique population of microorganisms. Strevett and Kibbey (2019) investigated nanomaterial interactions with bacteria and root surfaces in the rhizosphere and their impact on plant growth. A growth experiment was done by planting three buttercrunch lettuce seeds per centrifuge tube, three tubes per set of samples, and three different nanomaterials. The nanoparticles studied were titanium dioxide nanopowder, fluorescent red polystyrene latex nanospheres with sulfate surface functional groups, and fluorescent red polystyrene latex nanospheres with amine functional groups. According to Kibbey and Strevett (2019), the plants were watered twice daily using groundwater for the control and nanoparticles suspension for all other conditions in the morning and watering with groundwater for all samples in the afternoon. The results indicate that the stem and root length of the plant was affected by the nanoparticle suspension (Kibbey & Strevett, 2019). It was also found that the two systems with the highest impairment in growth had decreased rhizosphere bacterial counts, which means that the nanomaterials may be obstructing the plant growth by interfering with the growth or attachment of rhizosphere bacteria. Kibbey and Strevett (2019) suggested that nanoparticles cause changes in the bacterial surface properties by being attached to the bacteria surfaces and impacting the attachment of bacteria to root surfaces.

Zhou et al. (2020) studied the impact of TiO_2 and ZnO nanoparticles in soil bacteria. Their study aimed to reveal and compare the comprehensive effects of TiO_2 and ZnO on terrestrial plants, microorganisms, and the coexisting organic pollutant. It was found that ZnO exhibited an adverse ecotoxicological effect on soil

microorganisms, which changed with exposure time. Zhou et al. (2020) found that the addition of TiO_2 and ZnO resulted in a decrease of half of the genus found.

Mayton et al. (2019) studied the influence of copper oxide and titanium dioxide nanoparticles on the deposition and detachment of *Escherichia coli* in two model systems. Their study aimed to understand the aqueous interactions and transport of a specific foodborne pathogen and metal oxide nanoparticles. It was found by Mayton et al. (2019) that the charge of the particles was not affected by the copper oxide but got more negatively charged with the presence of titanium dioxide. Furthermore, the measured effective thermodynamic diameter of the suspensions reduced with the presence of nanoparticles compared to the bacteria alone.

2.3 Bacteria

Bacterial species are abundant in agriculture and mainly occur in soil particles, airborne spores, and irrigation water (Amarger, 2002). Those microbes can be beneficial as they are essential for decomposing organic matter to recycle old plant materials, drought tolerance, heat tolerance, and insect resistance (Barth et al., 2009). Thus, bacterial species maintain a dynamic ecological balance within agricultural systems.

Spoilage bacterial species are introduced to the fruits and vegetables during crop growth, harvest process, handling equipment, and storage. The spoilage microbes occurring in the fruits and vegetables are the same spoilage microorganisms that were presented in the harvesting and handling equipment in the packinghouse and storage facility. Vegetables are very close to the ideal conditions for bacterial species to survive and grow due to the nutrient richness and neutrality of pH levels (Barth et al., 2009). The ideal conditions encourage the spoilage microorganisms to exploit the host using

extracellular constituents as nutrients for their growth. The spoilage microorganisms exploit the host by using extracellular lytic enzymes that degrade their polymers to release water and the plant's other intracellular constituents to use as nutrients for their growth (Barth et al., 2009). Lytic enzymes are highly evolved molecules bacterial viruses produce to digest the bacterial cell wall. The ideal conditions for the microorganisms to spoil are dark areas with a temperature of 20 °C and above and 80-90% moisture (Barth et al., 2009).

Jackson et al. (2013) studied the bacterial community for organic and conventionally grown leafy salad vegetables at the point of consumption using both culture-dependent and culture-independent methods. They found that the most common bacterial species that occurs in spinach leaves are *Erwinia* sp. The bacterium *Erwinia* sp. is a highly effective spoilage microbe that infects and destroys plant tissues pre-and post-harvest, as well as causing frost injury to the spinach leaves (Amarger, 2002). *Erwinia* sp. is active only at temperatures greater than 20 °C; storing produce at a lower temperature will decrease them from growing and destroying the produce (Barth et al., 2009).

A study was made on *Erwinia*'s host range and total cellular protein fingerprint isolated from some vegetables in Egypt (Mikhail et al., 2019). The study included an identification test of *Erwinia*. Host range is the number of host species used by the pathogen. The objectives of their study were to identify the common *Erwinia* and study their difference in biochemical characters, host range, and protein fingerprints of Sodium Dodecyl Sulfate-PolyAcrylamide Gel Electrophoresis (SDS-PAGE) of total cellar proteins. SDS-PAGE is a fast method for detecting the differences among

bacterial species. The methods started with sampling and isolation. To achieve their purpose, the researchers used potato tubers, sweet potato roots, cucumber fruits, carrot roots, eggplant fruits, chili fruits, red sweet pepper fruits, and tomato fruits. The isolation procedure used a standard bacteriological method on 2% nutrient glucose (Mikhail et al., 2019). Their tests included tests to identify the pathogenicity and host range of *Erwinia* isolates, preparation of bacterial suspension, pathogenicity and host range procedures, and total cellular protein preparation of *Erwinia* isolates. The chemical tests revealed that *Erwinia* isolates differed in their fermentation ability of tested carbon sources producing acid only or acid and gas (Mikhail et al., 2019). They are also characterized by the high disease ability, as *Erwinia* can ferment many sugars within 24 hours.

2.4 Surface Energies

The concept of an attractive general interaction between neutral atoms was first proposed by van der Waals in 1873 to account for specific properties of nonideal gases and liquids (Van Oss et al., 1988). Surface energies are classified into high, low, and medium surface energies. High surface attractive energies occur when there is favorable interfacial thermodynamic attraction, resulting in negative Gibbs free energy. In the case of negative Gibbs free energy, the forces between surface molecules are attractive, resulting in wetting out and bonding. Low surface energy is when the surface molecules are weakly attracted to each other. Medium surface energy is when the surface molecules are between high and low surface energies. Orienting dipole-dipole interactions, randomly orienting dipole-induced dipole interactions, and fluctuating dipole-induced dipole interactions contribute to van der Waals interactions.

DLVO (Derjaguin, Landau, Verwey, and Overbeek) theory was created for macromolecules and particles, as it has been used to study the interactions involved in bacterial adhesion. The theory has been used to evaluate how interactions impact the adhesion and transport of nanomaterials and bacteria. Extended DLVO theory, a version of DLVO theory that includes Lewis acid-base interaction, was developed and successfully used to study bacterial adhesion. Lewis acid-base interaction was first defined as an acid or base substance that gives up or takes up hydrogen ions (Van Oss, 1994). Another definition introduced by Jenson (1978) is that acid and base in any given solvent would be the following: an acid is a substance that gives off a cation or combines with an anion of the solvent; a base is a substance that gives off an anion or combines with a cation of the solvent.

Warning et al. (2017) studied the mechanistic understanding of non-spherical bacterial attachment and deposition on plant surface structures. Their objective was to achieve a mechanistic understanding of the effect of plant topography and attachment. Warning et al. (2017) stated that drag and internal forces are significant forces on bacterial cells. Their model results found that trichomes decrease the local shear stress resulting in unfavorable attachment, excluding where the structures are perpendicular to the flow since shear stress is high. The results also indicated that stomata and grooves increase in attachment near the structures with high shear stress and shear stress gradient (Warming et al., 2017). Moreover, shear stress gradient and higher shear stress cause a shear-enhanced adhesion of bacteria.

Chen and Strevett (2001) studied the surface thermodynamics of bacteria. They discovered that as the bacteria approach the collector particles, the Lifshitz-van der

Waals and Lewis acid-base interactions increase with the decrease in distance between the surface. Chen and Strevett (2001) stated that the bacteria were repelled from the collector particles when the organisms approaches each other or the media at a distance more significant than the effective thickness of the electrical double layers due to the electrostatic force. The result of the study indicates that hydrodynamic forces and Brownian movements can overcome electrostatic repulsion. According to Chen and Strevett (2001), double layers were superimposed as the bacteria approached the collector particles, increasing the Lifshitz-van der Waals and Lewis acid-base interactions with a decreased distance between surfaces.

CHAPTER 3. MATERIALS AND METHODS

3.1 Materials

Baby spinach leaves were purchased periodically throughout the experiment from local stores. Seven different chemicals were used for preparing bacterial growth media, mannitol (MilliporeSigma CAS-No: 69-65-8), L-glutamic acid (MilliporeSigma CAS-No: 56-86-0), monopotassium phosphate (Fisher Scientific CAS-No: 7778-77-0), sodium chloride (MilliposeSigma CAS-No: 7647-14-5), magnesium sulfate heptahydrate (Mallinckrodt Baker CAS-No: 10034-99-8), yeast extract (MP Biomedicals CAS-No: 8013-01-2), LB broth (MilliposeSigma CAS-No: 7647-14-5), and agar (Fisher Scientific CAS-No: 9002-18-0). Autoclave, orbital shaker, incubator, and Benchtop Spectrophotometer (Hach DR3800) were also used for bacterial growth. The nanoparticles used in this study were Titanium dioxide (TiO2) nanopowder (P25 Aeroxide) obtained from Degussa Corporation (Düsseldorf, Germany). For measuring the contact angles, Formamide (MilliposeSigma CAS-No: 75-12-7), ethylene glycol (MillliposeSigma CAS-No: 107-21-1), and alpha bromonaphthalene (MilliposeSigma CAS No: 90-11-9) were used, along with two software TimedImage, and SenssileFit (created by personal communication).

3.2 Methods

3.2.1 Bacterial Growth

Spoilage bacteria were cultivated from rotting spinach. Fresh spinach was obtained from a local source and rotted for thirty days in a plastic bag to maintain humidity at 24^{o}C. Once appropriate spoilage occurred, the bacteria were cultivated with

growth media. The bacterial growth method was adapted from Seo et al. (2001). Primary growth media was LB media (Lysogeny broth) that was prepared by combining 10.0g of mannitol, 2.0g of L-glutamic acid, 0.5g of monopotassium phosphate (KH_2PO_4), 0.2g of sodium chloride (NaCl), 0.2g of magnesium sulfate heptahydrate ($MgSO_4.7H_2O$), 0.25g of yeast extract, and 15g of LB broth in one liter of distilled water. The media was dispensed in specialty Erlenmeyer flasks with a sidearm for measuring optical density and sterilized in a high temperature/pressure autoclave.

Aseptically, 10 mL of the liquid produced during the spinach spoilage process was added to each 250 mL media flask. The flasks were then incubated at 26°C in an orbital shaker. The culture was monitored, and optical density was measured every 100 minutes using the Hach device at a wavelength of 660nm. A growth curve was made, and the mid-growth stage was determined where the growth got at the highest since optical density is directly proportional to the dry weight of the bacteria.

3.2.2. Isolating Bacterial Consortiums

The bacterial isolation method was adapted from Pepper et al. (1995). The isolation started by preparing the agar with the same mixture from the LB media but adding 15.0 g of agar before autoclaving the isolation for 20 minutes and then pouring every 10 mL in a Petri plate and storing at a temperature of less than 6°C until it got solid texture. A dilution series was made following the Pepper et al. (1995) method with ratios of 1/100, 1/1000, 1/10000, and 1/100000, 0.1mL of each dilution was spread into a Petri plate with agar. The plates are then incubated at 26 °C for 48 hours. The colonies were selected from the plates, streaked in another Petri plate with agar, and incubated at

26 °C for one week. The isolation of bacterial streaks was completed to reduce the variability resulting from the consortium and study them individually.

The Gram reaction method was adapted from Pepper et al. (1995). A Gram reaction was done to identify the colonies where the bacteria will either stay purple (Gram-positive) or turn pink or red (Gram-Negative). Gram reaction was done by placing the picked colonies in a slide and applying a primary stain (crystal violet), followed by a mordant stain (Gram's iodine), and finally applying, decolorization with alcohol, acetone, or a mixture of both. The slide of the colony was then ready to be identified under a microscope. After studying the consortiums, the most common consortium was collected from the isolation plates. Those colonies were used as inoculum with LB media. Batch cultures were grown in a shake incubator at 26°C.

3.2.3. Contact Angles

Contact angle measurements were necessary to determine the surface tensions using the method provided in section 3.2.4. Contact angles were obtained for one isolated spoilage organism from above and one nanoparticle (titanium dioxide) using one apolar liquid (alpha-bromonaphthalene) and two polar liquids (formamide and ethylene glycol) to have 20 contact angles for each fluid on each surface. The contact angle measurement method was adapted from Chen and Strevett (2001). The method started with vacuum filtering 100 mL of the bacterial solution on a silver metal membrane until dried and ensured a multi-layer covering of the membrane. Contact angle measurements were used to quantify Lewis acid/base and Lifshitz-van der Waals

forces. Alpha-bromonaphthalene, formamide, and ethylene glycol were dropped on each surface to estimate their relevant cos θ.

3.2.4 xDLVO Model

Surface electrodynamic interactions were calculated using the contact angles, with an adapted method from Chen and Strevett (2001). Equation 1 is used to get the electron-donor γ_S^- and electron acceptor γ_S^+ parameters of the Lewis acid-base component of surface tension of the surface in units of mJ/m^2 (van Oss, 1994) as well as getting the Lifshitz-van der Waals γ_S^{LW} component of surface tension of the surface (L is for liquid and S is for surface). Where γ_L represents the surface tension of the liquid used:

$$(1 + cos\theta)\gamma_L = 2(\sqrt{\gamma_S^{LW}\gamma_L^{LW}} + \sqrt{\gamma_S^+\gamma_L^-} + \sqrt{\gamma_S^-\gamma_L^+}) \quad (1)$$

Finally, according to van Oss (1994), to obtain the Gibbs free energy for both Lifshitz-van der Waals interaction ΔG_{132}^{LW} and Lewis acid-base interaction ΔG_{132}^{AB} between micro-organisms, 1, and the spinach leaf, 2, immersed in water, 3 the following expressions (Equations 3 and 4) were used:

$$\Delta G_{132}^{LW} = -2(\sqrt{\gamma_3^{LW}} - \sqrt{\gamma_2^{LW}})(\sqrt{\gamma_3^{LW}} - \sqrt{\gamma_1^{LW}}) \quad (2)$$

$$\Delta G_{132}^{AB} = 2\sqrt{\gamma_3^+}\left(\sqrt{\gamma_1^-} + \sqrt{\gamma_2^-} - \sqrt{\gamma_3^-}\right) + 2\sqrt{\gamma_3^-}\left(\sqrt{\gamma_1^+} + \sqrt{\gamma_2^+} - \sqrt{\gamma_3^+}\right) - 2\sqrt{\gamma_1^+\gamma_2^-} - 2\sqrt{\gamma_1^-\gamma_2^+} \quad (3)$$

3.2.5. Bacterial Growth in the Presence of Titanium Dioxide

A growth experiment was necessary to determine the number of bacterial consortiums attached to the spinach leaves with and without nanoparticles. Eight fresh

spinach leaves were used with approximately the same leaf area following the Montgomery equation adopted from He et al. (2020). The equation used is:

$$A = c_1 LW \quad (4)$$

Where c_1 is the Montgomery parameter which equals $\frac{\pi}{4}$, as L is the length and W is the width of the leaf. The length and width were determined used caliper measuring tool. The standard deviation and standard error were calculated using the following equations:

$$\sigma = \sqrt{\frac{\sum(x_i-\mu)^2}{N}} \quad (5)$$

Where σ is the standard deviation, x_i is each value from the population, μ is the population mean, and N which is the size of populations.

$$SE = \frac{\sigma}{\sqrt{n}} \quad (6)$$

Where SE is the standard error and n is the number of samples. Seven leaves were dipped into different concentrations of titanium dioxide nanoparticles. The samples were left in a dark, humid container at 24°C to maintain 100% relative humidity and promote rotting. The concentration of titanium dioxide nanoparticles used includes three environmentally relevant concentrations, 0.05 g/L, 0.1 g/L, and 0.5 g/L, and four non-environmentally relevant 10.5 g/L, 16.8 g/L, 25.2 g/L, and 31.5 g/L. After rotting, both spinach leaves were diluted following a standard serial dilution method (Pepper et al., 1995) with ratios of 1/1000 and 1/10000, followed by the transfer of 0.1 mL to a streak plate. The streak plates were then incubated at a temperature of 26 °C for seven days. The experiment was repeated four times to investigate the reproducibility of the results.

3.2.6 Statistical Analysis

Statistical analysis was applied for bacterial colonization in the presence of titanium dioxide results. The *t*-test method was adapted from Kim (2015) to compare the titanium dioxide concentrations with each other. This statistical analysis was chosen since the sample size is small and provides a method of determining the 95% confidence interval (95% CI). One-tailed distribution and paired type were used to determine whether a significant change occurred in the decrease of bacterial growth with the addition of titanium dioxide concentration (Kim, 2015). This statistically significant difference between the means of two bacterial growth values is determined by calculating the probability (p-value). The p-value is the probability of the statistical test where the growth between two TiO_2 concentrations is different. If the p-value is less than 0.05, a statistical difference occurs. While if the p-value is higher than 0.05, no statistical difference occurs.

CHAPTER 4. RESULTS AND DISCUSSION

The results are discussed in five sections, including bacterial growth, isolating bacterial consortiums, electrodynamic energies, bacterial growth in the presence of titanium dioxide, and statistical analysis. Bacterial growth results include spinach spoilage, bacterial growth using LB media, and rotten spinach slime. Isolating bacterial consortiums include colony Gram reaction and *Erwinia* growth in LB media. Electrodynamic energy results include contact angle measurement, surface tension, and Gibbs free energy values. Finally, bacterial growth in the presence of titanium dioxide results includes bacterial growth with different concentrations of titanium dioxide. The statistical analysis includes a t-test of bacterial growth with titanium dioxide.

4.1. Bacterial Growth

For isolating spoilage bacteria from spinach leaves, spinach leaves were placed in a dark and secured plastic bag to maintain humidity at a temperature of 25 °C for 35 days (Figure 4.1). Figure 4.1 shows three different time steps from the initial (0 days, Figure 4.1A) to 11 days (Figure 4.1B) and finally at 35 days (Figure 4.1C). By reaching day 11, the spinach leaves color turned a darker shade of green and then eventually turned brown with visible extracellular production. The presence of brown slime became more predominant on the leaves by the end of the experiment 35 days later. Slimy moisture is a by-product of microorganisms. This material resulted from microorganisms using the plant's cellular lytic enzymes to release water and other intracellular constituents to use as nutrients for their growth (Barth et al., 2009).

Different microorganisms were expected to be found on the rotten spinach leaves. According to Jackson et al. (2013), it was expected to find *Erwinia*,

Flavobacterium, Janthinobacterium, and *Serratia* in rotten spinach leaves. *Erwinia* was targeted for isolation since it has been reported to be the dominant bacterial species in spinach leaves (Jackson et al., 2013). An LB media was prepared to cultivate those microorganisms to provide the protein and nitrogen nutrition needed. 10 mL per sample of rotten spinach slime was then added to the LB media. After growing the organisms in an orbital shaker, the optical density was measured every one to two hours to keep track of the growth. The microorganism's growth was completed after 14 hours. Optical density was used to create a growth curve and determine the mid-growth phase (Appendix Figure 1). This phase was targeted since it corresponds to the highest optical density and, therefore, the highest bacterial population. The highest stable optical density was 2.15, corresponding to a 16g/L dry weight. The dry weight was measured by vacuum filtration.

Figure 4.1 Spinach Rot Stages with Day 0 (A), Day 11 (B), and Day 35 (C)

4.2 Isolating bacterial consortiums

Bacterial growth started to occur after three days of incubation. The bacterial colonies were then picked and streaked on LB agar to grow in an incubator for seven days. Individual colonies were selected for Gram reaction. A Gram reaction was done to identify the colonies where the bacteria will either stay purple (Gram-positive) or turn pink or red (Gram-Negative), where it was identified as likely being *Erwinia* species (Figure 4.2). *Erwinia* is a Gram-negative *Bacillus* (Gilardi et al., 1970). Finding the dominant bacterial species is likely *Erwinia* was consistent with previously reported research (Jackson et al., 2013). Jackson et al. (2013) identified that *Erwinia* sp. was the most common bacterial species extracted from spinach leaves as it represents more than 60% of the total bacterial populations found in spinach leaves. Although the identification of *Erwinia* in this work is not confirmed, the bacteria isolated in this work will be referred to as *Erwinia* for the remainder of this thesis in the interest of conciseness.

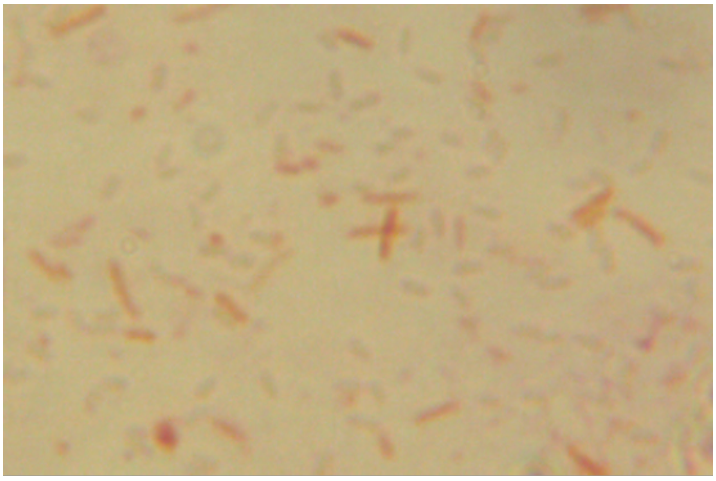

Figure 4.2. *Erwinia* sp. Gram-negative Reaction having a Bacillus morphology.

To prepare the *Erwinia* species for contact angle measurements, isolated colonies from agar plates were aseptically transferred to LB growth media. Although LB broth is the preferred growth media, low biomass production was observed. A dry weight of *Erwinia* was measured to be 0.116 g/L, which was not enough to have a multi-layer of bacteria on the silver membrane. In microbiology, catabolism is a chemical reaction that converts substrates into lower-energy products. The electron donor in this reaction is taken as a carbon or nitrogen source for the anaerobic reaction that converts it into cell biomass (Gonzalez-Cabaleiro et al., 2015). For investigating possible causes of low biomass production, the impact of the increased carbon source was studied. The primary carbon source in LB broth is mannitol. Additional batch growth using a 20 g/L concentration of mannitol resulted in a 20.5% decrease to reach 0.092 g/L in biomass production as measured by dry weight.

It was found that the growth rate and yield usually decrease with the increase of carbon source (Ellis et al., 2000). Ellis et al. (2000) stated no connection between growth rate and carbon source concentration. An inverse relationship between growth rate and biomass density was observed, as increased carbon source concentration slightly reduced the biomass concentration. Since the additional carbon source did not increase biomass, attention was then turned to the bioavailability of the nitrogen source. The primary nitrogen source in LB broth is yeast extract. Subsequent enrichment included increased yeast extract to augment any nutrient limitation that did succeed in raising biomass production to 0.82 g/L.

A growth was done by doubling the yeast extract in eleven days to have full growth (Figure 4.3). There are four distinct phases of bacterial growth. The first phase

is the lag phase, which occurs at the beginning of the growth curve, where the bacteria are acclimating to the available metabolites. During this phase, the catabolic metabolism is very active as bacteria develop the enzymatic infrastructure for anabolism. The following exponential growth phase is a period of rapid cell growth. During this phase, the carbon is shunted through the anabolic metabolic pathways resulting in increased biomass production. Following is the stationary phase; during this phase, the cell reproduction gets slower and equal to the amount of cell death due to the unideal conditions for reproduction resulting in a change of metabolic activity. The death phase comes last, where living cells stop metabolic functions and begin the death process (Zwietering et al., 1990).

The Monod equation represents a smooth transition from a first-order relationship at low substrate concentration to a zero-order relationship at high substrate concentration. According to Monod's model, the specific growth rate is related to the concentration of a rate-limiting electron-donor substrate (Rittmann et al., 2020). The author tested the *Erwinia* growth rate for different temperatures, as the best growth rate has been reported to occur at temperatures between 25^{o}C and 30^{o}C (Billing, 1974). The specific growth rate for *Erwinia* was 0.046 h^{-1} at a temperature of 26^{o}C, which was in the same range as Billing (1974) values of *Erwinia* growth.

The best-fit curve was used to show the batch growth curve. A second-order polynomial trendline was the best fit to represent the growth curve shape. Figure 4.3 illustrate a strong positive Pearson correlation coefficient. *Erwinia's* growth curve does confirm Byers et al. (2002) observations of long growth. The main reason for the growth time differences is the different media types (Pepper et al., 1995). The mid-

growth needed to be targeted for the contact angle measurements to ensure a multi-layer lawn of bacteria. The highest bacterial dry weight was found in mid-growth on day 8 (Figure 4.3).

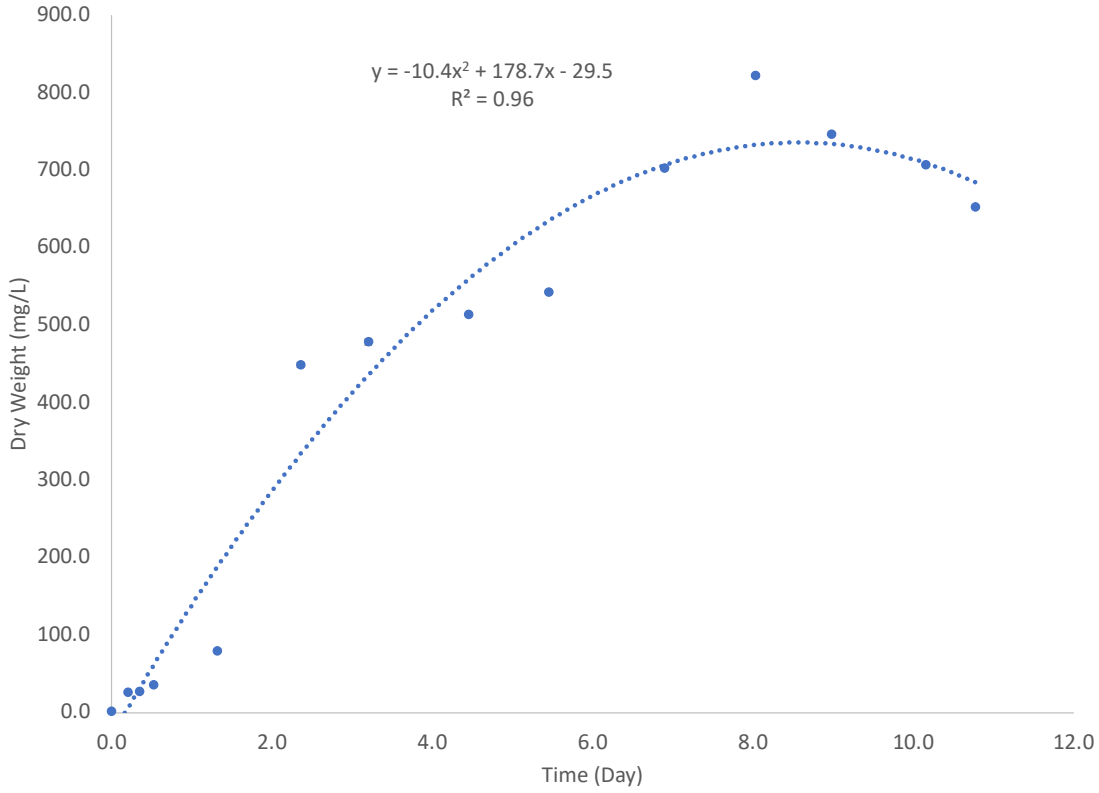

Figure 4.3. Growth Curve of *Erwinia* Bacteria Represented as Time (day) vs Dry Weight (mg/L)

4.3 Electrodynamic Energies

A 100 mL *Erwinia* solution was vacuum filtered using a 0.45 µm pore size silver membrane to obtain a multi-layer lawn of bacteria. The target dry weight of this bacterial layer was 0.80 ± 0.05 g. This mass was used to ensure complete coverage of the silver membrane. The bacterial layer was then ready for the contact angle measurement. A drop of 5 µm of water, ethylene glycol, or alpha-bromonaphthalene was placed on the lawn of bacteria. Note that earlier work with fresh spinach used

formamide instead of water immediately after each fluid was placed on the bacterial layer. An image using TimedImage software was captured. The images were fitted into SessileFit software to get the contact angle (θ) values. Figure 4.4 demonstrates how SessileFit software fits the angle to get the most accurate contact angle.

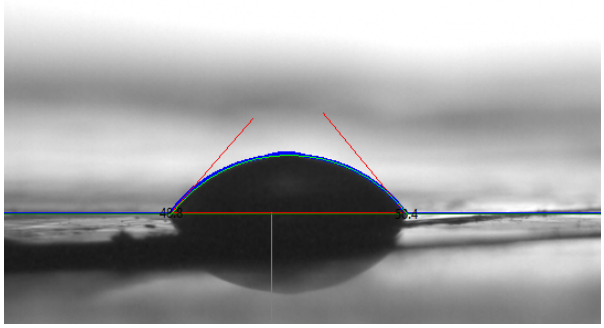

Figure 4.4. Contact Angle Fit using SessileFit Software.

Measured contact angle values can be found in Table 1 and Table 2 of the appendix, while average values are shown in Table 4.1. Values in Table 4.1 illustrates each fluid's average contact angles between the 40th and 60th percentiles on fresh spinach and *Erwinia*. 40th and 60th percentiles were chosen due to the roughness of the surfaces studied.

Table 4.1. Average Contact Angles (θ) values for *Erwinia* and Fresh Spinach express in unit of degree.

	Water	Ethylene glycol	Alpha Bromonaphthalene	Formamide
Erwinia	26.9	29.8	51.5	N/A
Fresh Spinach	N/A	59.8	48.2	69.7

The contact angles were used to determine the γ_s^{LW}, γ_s^+, and γ_s^- from Equation 2. After calculating the surface tensions of *Erwinia,* the average value of the electron-donor parameter γ_s^- was three times higher than any other bacterial values recorded by Chen and Strevett (2002).

Surface tension components of *Erwinia* were determined using contact angle values that can be reviewed in Table 1 of the appendix. The final average values of the Lifshitz-van der Waals component, electron donor, and electron acceptor of Lewis acid/base are illustrated in Table 4.3. The spinach leaf surface tension values (γ^{LW}, $\gamma^+$and γ^-) were obtained from a previous study (Kibbey T., unpublished data, 2022) and presented in Table 4.2. The method for fresh spinach was the same as *Erwinia* contact angles used of different fluids, as noted previously.

The water γ^{LW} value used was 21.8 mJ/m^2 (Chen & Strevett, 2002; Araujo et al., 2010). The $\gamma^+$and γ^- equal 25.5 mJ/m^2 (Chen & Strevett, 2002; Araujo et al., 2010). The γ^{LW} of alpha-bromonaphthalene equals 44.4 mJ/m^2 while $\gamma^+$and γ^- both equal 0.0mJ/m^2 (van Oss, 1988; Araujo et al., 2010). Van Oss (1993) and Araujo et al. (2010) also stated that the γ^{LW} of ethylene glycol equals 29 mJ/m^2, γ^+ equals 1.92 mJ/m^2, and γ^- to equal 47mJ/m^2.

Table 4.2 γ_s^{LW} of *Erwinia* corresponds with the range of Chen and Strevett (2002) for *Pseudomonas,* where they got a value of 34.2 mJ/m^2 for γ_s^{LW}. The γ_s^+ and γ_s^- of *Erwinia* also correspond with the range of Chen and Strevett (2002) for *Pseudomonas,* where they got a value of 0.59 mJ/m^2 for $\gamma_s^+$and 59 mJ/m^2 for γ_s^-. *Erwinia* values of surface tension in Table 4.3 also correspond with Azeredo et al. (1999), where that study measured the surface tension components of *S. paucimobilis* to

evaluate the bacterial adhesion to a glass coated with excrete polymeric substances where the results are similar to the values of surface tension measured for *Erwinia* (Table 4.2). Azeredo et al. (1999) that the Lifshitz-van der Waals interfacial surface tension γ_s^{LW} is 27.4 mJ/m^2. Lewis acid-base interfacial surface tension γ_s^+ is 1.0 mJ/m^2, and γ_s^- is 63.5 mJ/m^2, which confirms *Erwinia* surface tension shown in Table 4.2 that was used to measure Gibbs free energy.

While no studies were found regarding fresh spinach surface tension components, γ_s^{LW} and γ_s^+ of fresh spinach are very close to the *Erwinia.* At the same time, γ_s^- is much lower compared to the *Erwinia* value and Chen and Strevett (2002) surface tension of sand grains. Bayoudh et al. (2006) stated that when γ_s^- was higher than γ_s^+, the surface would be predominantly electron-donating, which can be seen in *Erwinia* values in Table 4.2.

Table 4.2. Average surface tension parameters. Error ranges correspond to calculated standard deviations.

	γ_s^{LW} (mJ/m^2)	γ_s^+ (mJ/m^2)	γ_s^- (mJ/m^2)
Erwinia Average values	29.23 +/- 0.24	0.47 +/- 0.16	63.39 +/- 1.81
Spinach Leaves Average values	30.62 +/- 0.31	0.68 +/- 0.07	6.35×10^{-15} +/- 8.44×10^{-15}

The Gibbs free energies were then computed using equations 2 and 3. The Gibbs free energy for Lifshitz-van der Waals interaction between *Erwinia* and the spinach leaf ΔG_{132}^{LW} equals -1.27 mJ/m^2, and the Gibbs free energy for Lewis acid-base interactions

between *Erwinia* and the spinach leaf equals -1.94x10^{-1} mJ/m^2. That gives a total ΔG_{132}^{LW+AB}= -20.71 mJ/m^2. Negative Gibbs free energy for Lifshitz-van der Waals indicates a net attraction (attractive interaction). It also indicates that interaction is a favorable interfacial thermodynamic attraction resulting in molecules bonding quickly. Negative Gibbs free energy for Lewis acid-base indicates that the *Erwinia* can potentially adhere to the fresh spinach leaves. The Gibbs free energy values correspond with Chen and Strevett (2002) values. Their Gibbs free energy interactions between different microorganisms and the silica gel were negatively charged for both Lifshitz-van der Waals and Lewis acid-base interactions. Negative Gibbs free energy also corresponds with Araujo et al. (2010). Araujo et al. (2010) recorded negative Gibbs free energy for *Pseudomonas* to study microbial adhesion.

Between *Erwinia* and titanium dioxide Gibbs free energy for both Lifshitz-van der Waals and Lewis acid-base was also calculated. Surface tension parameters for titanium dioxide were adapted from Huang et al. (2015) as γ_s^{LW}= 29.8 mJ/m^2, γ_s^+ = 5.5 mJ/m^2, and γ_s^-= 47.5 mJ/m^2. Furthermore, ΔG_{132}^{LW} calculated to be -1.16 mJ/m^2, and ΔG_{132}^{AB} equals 31.82 mJ/m^2, giving a total ΔG_{132}^{LW+AB}= 30.65 mJ/m^2. Because this value is positive, the Lifshitz-van der Waals and Lewis acid-base interactions produce a repulsive force between bacteria and titanium dioxide.

Comparing the total Gibbs free energies gives an initial possibility that *Erwinia* would be more attractive to the spinach leaf without titanium dioxide. As well as expecting bacterial growth to drop with titanium dioxide. Bayoudh et al. (2006) studied the Gibbs free energy between bacteria and hydrophobic and hydrophilic substrata. Their study found Gibbs free energy between *Staphylococcus epidermidis* and

hydrophobic glass surface was negative for Lifshitz-van der Waals and positive for Lewis acid-base.

Biosurfactants can play a role in improving the surface interactions. According to Shekhar et al. (2015), biosurfactants can enhance hydrocarbon bioremediation by increasing the substrate bioavailability for microorganisms. Biosurfactants can also increase the hydrophobicity of the surface, allowing hydrophobic substrates to associate more readily with bacterial cells. *Erwinia* is a biosurfactant-producing bacteria that can improve surface interactions (Shekhar et al., 2015).

4.4. Bacterial Growth in the Presence of Titanium Dioxide

A study of the impact of titanium dioxide on growth colonization on fresh spinach leaves was repeated three times for confirmation. The average area of spinach leaves was 14.1 cm^2, with a standard deviation of 0.29 and a standard error of 0.064. The results are presented in Figures 4.5 and 4.6, where the low titanium dioxide concentrations did not impact the bacterial growth with a standard deviation bar. In contrast, increased titanium dioxide concentrations resulted in a decreased colony-forming unit (CFU) for higher TiO_2 concentrations. The average number of colonies grown to have 0 g/L titanium dioxide is $38x10^4$ CFU/mL, equal to 0.05 g/L of titanium dioxide. The number of colonies slightly decreased, reaching $37x10^4$ CFU/mL for both 0.1 g/L and 0.5 g/L concentrations of titanium dioxide.

Moreover, the number of colonies grown was reduced to $18x10^4$ CFU/mL by adding 10.5g/L of titanium dioxide (Figures 4.5 and 4.6). There was $8x10^4$ CFU/mL in

the presence of 16.8 g/L of titanium dioxide. CFU decreased to $6x10^4$ CFU/mL for 25.2g/L and $2x10^4$ CFU/mL for 31.5g/L (Figures 4.5 and 4.6).

These results were similar to those reported by Chavan et al. (2020). In their study, Chavan et al. (2020) investigated the effects of titanium dioxide on plant growth-promoting bacteria from soil. A reduction in *Arthrobacter, Bacillus, Pseudomonas,* and *Klebsiella* numbers was observed when adding titanium dioxide at concentrations between 100-700 µg/L (Chavan et al., 2020). Their results confirm the relationship illustrated in Figure 4.5 for high concentrations of TiO_2, although the results presented herein are much higher concentrations than those used by Chavan et al. (2020).

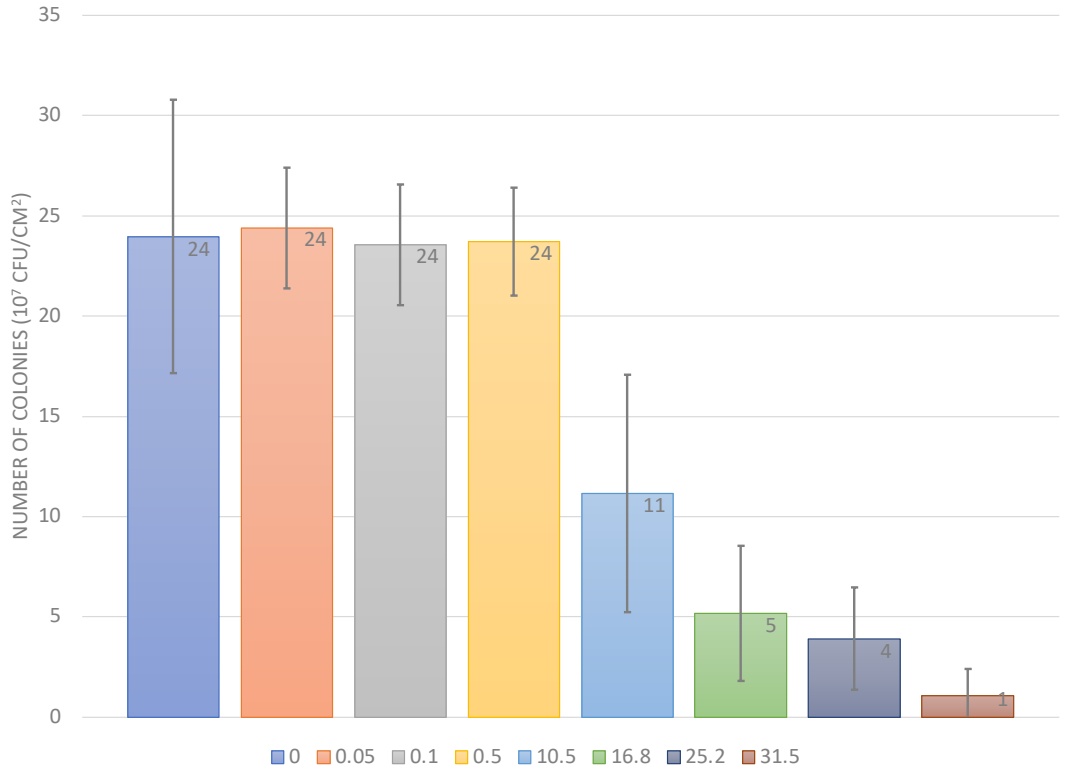

Figure 4.5. Number of Bacterial Colonies Grown in Eight Different Concentration of Titanium Dioxide (TiO_2).

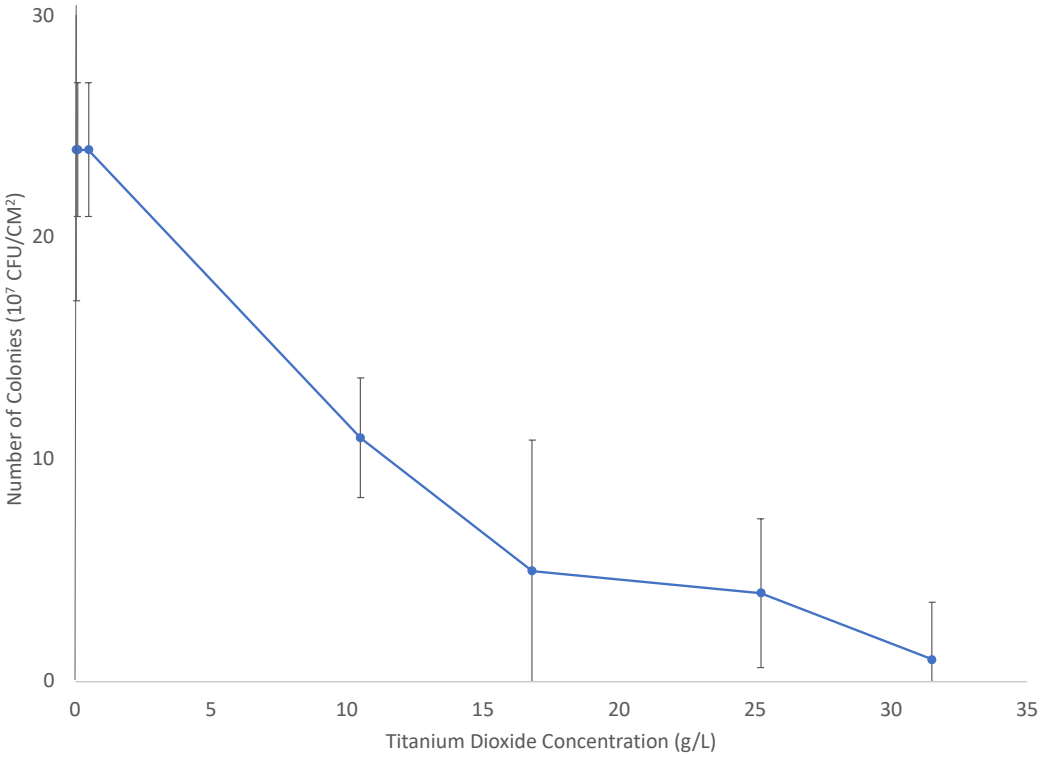

Figure 4.6. The Change in the Number of Colonies (10^4 CFU/mL) with the Increase of TiO_2 Concentration (g/L)

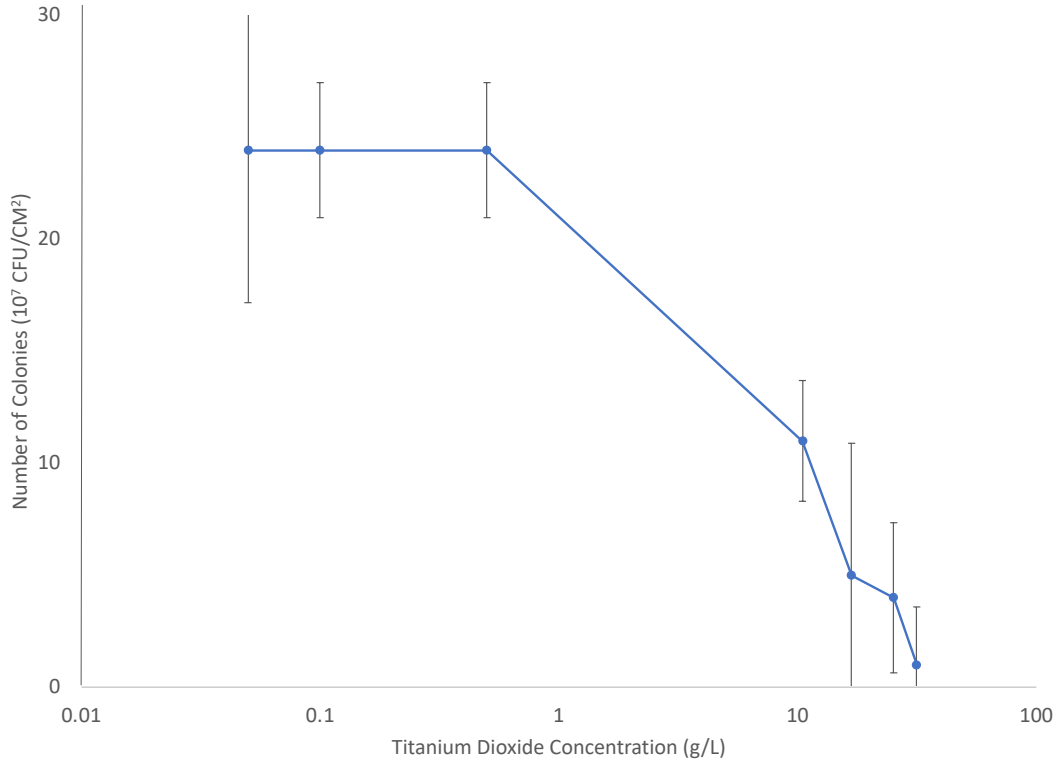

Figure 4.7. The Change in the Number of Colonies (10^4 CFU/mL) with the Increase of TiO_2 Concentration (g/L)

4.5 Statistical Analysis

The statistical analysis was done for the eight different titanium dioxide concentrations in Figure 4.5. The p-value is the probability of the statistical test where the growth between two TiO_2 concentrations is different. The results of a probability larger than 0.05 do not have a significant difference, whereas a probability less than 0.05 have a significant difference with a 95% confidence interval. Figure 4.8. illustrates the significant changes in bacterial growth with the different TiO_2 concentrations as colored cells.

Moreover, the p-values can be reviewed in Tables 3 and 4 in the appendix. The p-values confirmed the relationship of Figure 4.5, where the high p-values occur between the lower titanium dioxide concentrations which are environmentally relevant. In comparison, lower p-values occur between higher titanium dioxide concentrations, which are non-environmentally relevant. However, a significant difference occurs in the non-environmentally relevant titanium dioxide concentrations (95% CI). This difference did support the hypothesis that titanium dioxide reduces the growth of spoilage bacteria on spinach leaves.

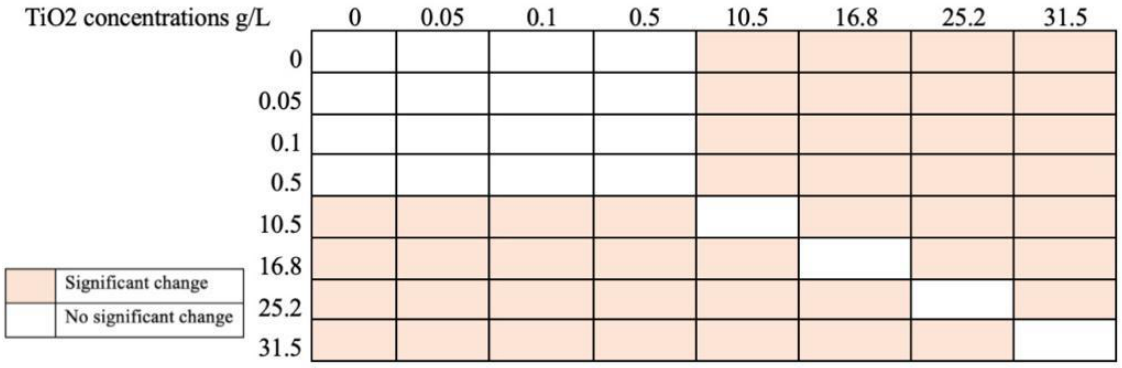

Figure 4.8. Significant Changes Occurrences in Bacterial Growth with Different TiO_2 Concentrations.

CHAPTER 5. CONCLUSION AND RECOMMENDATIONS

This work aimed to isolate spoilage bacteria from spinach leaves, determine the surface thermodynamic energies of bacteria isolates, evaluate the impact of nanoparticles on bacterial attachment from leafy vegetables, and determine the changes in Lifshitz-van der Waals and Lewis Acid/Base interfacial forces of bacteria in the surface with and without the presence of nanoparticles. It was hypothesized that titanium dioxide reduces the growth of spoilage bacteria on spinach leaves. The methods were divided into five sections: bacterial growth, isolating bacterial consortiums, contact angle, model development, and bacterial growth with the presence of titanium dioxide.

Spinach spoilage took 35 days to form; LB media was used then for bacterial growth as the most recognized bacteria found was likely to be the *Erwinia* species. *Erwinia* growth was done using LB media, where the mid-growth was targeted after eight days. Furthermore, the Gibbs free energy between *Erwinia* and fresh spinach leaves for both Lifshitz-van der Waals and Lewis acid-base interactions with spinach leaves was calculated to be negative. Negative Gibbs free energy interactions indicate a favorable interfacial thermodynamic interaction, and *Erwinia* adheres to spinach leaves. Gibbs free energy was also calculated for Lifshitz-van der Waals and Lewis acid-base between *Erwinia* and titanium dioxide. This calculation resulted in a negative value for Gibbs free energy for Lifshitz-van der Waals and a positive value for Lewis acid-base. A comparison was made between Gibbs free energy values of *Erwinia* and spinach leaves and between *Erwinia* and TiO_2, which indicates the possibility that *Erwinia* would be more attractive to the spinach leaf without titanium dioxide. Moreover, the

bacterial growth in the presence of titanium dioxide resulted in a reduction in the colony-forming unit after increasing titanium dioxide concentrations. A significant change was proven by the statistical analysis with 95% CI between bacterial growth and high concentrations of TiO_2.

It is recommended to calculate electrostatic energy for *Erwinia*, fresh spinach leaves, and titanium dioxide to better understand surface energy. Using a variation of nanoparticles can also support understanding the reason behind the reduction in bacterial growth.

REFERENCES

Abdulhameed M. F., Taha A. A., and Ismail R. A. (2021). *Influence of Cerium Oxide Nanoparticles and NPK Nanofertilizers on Growth and Yield of Cabbage Plant.* Plant Archives Vol. 21. PP 1326-1331.

Amarger M. (2002). *Genetically Modified Bacteria in Agriculture.*

Araujo E. A., de Andrade N. J., da Silva L. H. M., de Carvalho A. F., de Sa Silva C. A., and Romas A. M. (2010). *Control of Microbial Adhesion as a Strategy for Food and Bioprocess Technology.* Food Bioprocess Technology Vol. 3 PPP. 321-332.

Azeredo J., Visser J., and Oliveira R. (1999). *Exopolymers in Bacterial Adhesion: Interpretation in Terms of DLVO and XDLVO theories.* Colloids and Surfaces B: Biointerfaces Vol. 14. PP 141-148.

Bai F., Che Y., Kami-ike N., Ma Q., Minamo T., Sowa Y., and Namba K. (2013). *Population Heterogeneity vs. Temporal Fluctuation in Escherichia coli Flagellar Motor Switching.* Biophysical Journal Vol. 105.

Barth M., Hankinson T.R., Zuang H., Breidt F. (2009). *Microbiological Spoilage of Fruits and Vegetables.*

Bayoudh A., Othmane A., Battaieb F., Ben Ouda H., and Ponsonnet L. (2006). *Quantification of the Adhesion Free Energy Between Bacteria and Hydrophobic and Hydrophilic Substrata.* Material Science and Engineering C Vol. 26 PP. 300-306.

Billing E. (1974). *The Effect of Temperature on Growth of the Fireblight Pathogen, Erwinia amylovora.* Jornal of Applied Bacteriology Vol. 37 PP. 643-648.

Boeses S. R. and Hunter N. P. (1990). *Effect of Growth Temperature and Temperature Shifts on Spinach Leaf Morphology and Photosynthesis.* Plant Physiol. Vol. 94 PP. 1830-1836.

Byers J. T., Lucas C., Salmonf G. P. C., and Welch M. (2002). *Nonenzymatic Turnover of an Erwinia carotovora Quorum-sensing signaling Molecule*. American Society of Microbiology Vol.184 PP.1163-1171.

Chaudhary I. and Singh V. (2020). *Titanium Dioxide Nanoparticles and its Impact on Growth, Biomass and Yield of Agricultural Crops under Environmental Stress.* Research Jornal of Nanoscience and Nanotechnology. 10(1):1-8.

Chavan S., Sarangdhar V., and Nadanathangam V. (2020). *Toxixological effects of TiO_2 Nanoparticles on Plant Growth Promoting Soil Bacteria.* Emerging Contaminants Vol. 6 PP. 87-92.

Chen G., and Strevett K. (2001). *Impact of surface thermodynamics on bacterial transport.* Environmental Microbiology. Vol. 3 PP 237-45.

Chen G., and Strevett K. (2002). *Microbial Surface Thermodynamics and Interactions in Aqueous Media.* Jornal of Colloid and Interface Science Vol. 261. PP. 283-290.

Elis B. D., Butterfield P., Jones W. L., McFeters G. A., and Camper A. K. (2000). *Wffects of Carbon Source, Carbon Concentration, Chlorination on Growth Related Parameters of Biofilm Bacteria.* Microbial Ecology Vol. 38 PP. 330-347.

Gilardi G. L., Bottone E., and Bimbaum M. (1970). *Unusual Fermentative, Gram-Negative Bacilli Isolated from Clinical Specimens.* Applied Microbiology Vol. 20 PP. 151-155.

Gonzalez-Canaleiro R., Ofiteru I. D., Lema J. M., and Rodriguez J. (2015). *Microbial Catabolic Activities are Naturally Selected by Metabolic Energy Harvest Rate.* The ISME Journal Vol. 9 PP. 2630-2641.

Hassan A. N., and Frank J.F. (2002). *Influence of surfactant hydrophobicity in the detachment of Eschrichia coli O157:H7 from lettuce.* International Journal of Food Microbiology Vol.87. PP. 145-152.

He J., Reddy G., Liu M., and Shi P. (2020). *A General Formula for Calculating Surface Area of the Similarly Shaped Leaves: Evidence from Six Mangoliaceae Species.* Global Ecology and Conservation Vol. 23.

Huang G., Zia D., Ng T., Yip H., Li G., Zhao H., and Wong P. (2015). *Dual Roles of Capsular Extracellular Polymeric Substrances in Photocatalytic Inactivation of Escherichia coli: Comparison of E. coli BW25113 and Isogenic Mutants.* Applied and Environmental Microbiology Vol. 81 PP. 5174-5183.

Jackson C. R., Randolph K. C., Osborn A. L., and Tyler H. L. (2013). *Culture Dependent and Independent Analysis of Bacterial Communities Associated with Commercial Salad Leaf Vegetables.* BMC Microbiology 13:274.

Jensen W. B. (1978). *Lewis Acid-Base Definitions: A Status Report.* Chemical Reviews.

Kibbey T. C. G., and Strevett K. A. (2019). *The Effect of Nanoparticles on Soil and Rhizosphere Bacteria and Plant Growth in Lettuce Seedlings.* Chemosphere Vol. 221 PP. 703-707.

Kim T., (2015). *Statistical Round*. Korean Journal of Anesthesiology Vol. 6 PP. 540-546

Kioke S. T., Cohn M., and Cantwell M. (2011). *Spinach Production in California.* UC Agriculture & Nature Resources. Vol. 7212.

Li B. and Logan B. E. (2004). *Bacterial Adhesion to Glass and Metal-Oxide Surfaces*. Colloids and Surfaces B: Biointerfaces Vol. 36. PP.81-90.

Mayton H. M., White D., Marcus I. M., and Walker S. L. (2019). *Influence of nano-CuO and -TiO_2 on Deposition and Detachment of Escherichia coli in Two Model Systems.* Environmental Science Nano Vol. 6 PP. 3268-3279.

McNear D. H. (2013). *The Rhizosphere-Roots, Soil, and Everything In Between.* Nature Education Knowledge 4(3):1.

Naznin M. T., Lefsrud M., Gravel V., and Kalam Azad M. O. (2019). *Blue Light Added with Red LEDs Enhance Growth Characteristcs, Pigments Content, and Antioxidant Capacity in Lettuce, Spinach, Kale, Basil, and Sweet Pepper in Controlled Environment.* Plants Vol. 8.

Pepper I.L., Gerba C.P., and Brendecke J.W. (1995). *Environmental Microbiology: A Laboratory Manual*. Academic Press. PP. 21-33.

Pestovsky Y. S., and Matrinez-Antonio A. (2017). The Use of Nanoparticles and Nanoformulations in Agriculture. Journal of Nanoscience and Nanotechnology Vol. 17. PP. 8699-8730.

Rittman B. E., and McCarty P. L. (2020). *Environmrntal Biotechnology: Principles and Applications* (second eddition). McGraw-Hill Education.

Seo S.T., Furuya N., Lim C. K., Takanami Y., and Tsuchiya K. (2011). *Phenotypic and Genetic Diversity of Erwinia carotovora ssp. carotovora Strains in China.* Blackwell Wissenchafts-Verlag, Berlin Vol. 150. PP. 120-127.

Shaker S., Sundaramanickam A., and Balasubramanian T. (2015). *Biosurfactant Producing Microbes and their Potential Applications: A Review.* Critical Reviews in Environmental Science and Technology Vol. 45 PP. 1522-1554.

Toth I. K., Bertheau Y., Hyman L.J., Laplaze L., Lopez M.M., McNicol J., Niepold F., Persson P., Salmond G. P. C., Sletten A., van der Wolf J. M., and Perombelon M. C. (1999). *Evaluation of Phenotypic and Molecular Typing Techniques for Determining Diversity in Erwinia carotovora subspp. Atroseptica.* Journal of Applied Microbiology Vol.87. PP. 770-781.

Van Oss C. J. (1988). *Energetics of Cell-Cell and Cell-Biopolymer Interactions.*Humana Press Inc. Vol. 14.

Van Oss C. J. (1993). *Acid-base Interfacial Interactions in Aqueous Media.*Colloids and Sufaces A: Physicochemical and Engineering Aspects Vol. 78.

Van Oss C. J. (1995) *Hydrophobicity of biosurfaces- origin, quantitative determination, and interaction energies.* Colloids and surfaces B: Biointerfaces 5.3-4(1995): 91-110.

Van Oss C. J. (1994) *Interfacial Forces in Aqueous Media,* Marcel Dekker, New York.

Van Oss C. J., Chaudhury M. K., and Good R. J. (1988). *Interfacial Lifshitz van der Waals and Polar Interactions in Macroscopic Systems*. Chemical Reviews Vol. 88. PP. 927-941.

Warning A. D., and Datta A. K. (2017). *Mechanistic Understanding of Non-spherical Bacterial Attachment and Deposition on Plant Surface Structures.* Chemical Engineering Sience Vol. 160 PP. 396-418.

Wu W., Giese Jr. R. F., and van Oss C. J. (1995) *Evaluation of the Lifshitz van der Waals/Acid-Base Approach to Determine Surface Tension Components*. Langmuir Vol. 11. PP. 378-379.

Zhou Q., Zhang X., and Wu Z. (2020). *Impact of TiO_2 and ZnO Nanoparticles on Soil Bacteria and the Enantioselective Transformation of Racemic-Metalaxyl in Agricultural Soil with Lolium Perenne: A Wide Greenhouse Cultivation.* Jornal of Agricultural and food chimestry Vol. 6 PP. 3268-3279.

Zwietering M. H., Jongenburger I., Rombouts F. M., and Vantrient K. (1990). *Modeling of the Bacterial Growth Curve.*Applied and Environmental Microbiology Vol. 56 PP. 1875-1881.

APPENDIX A:

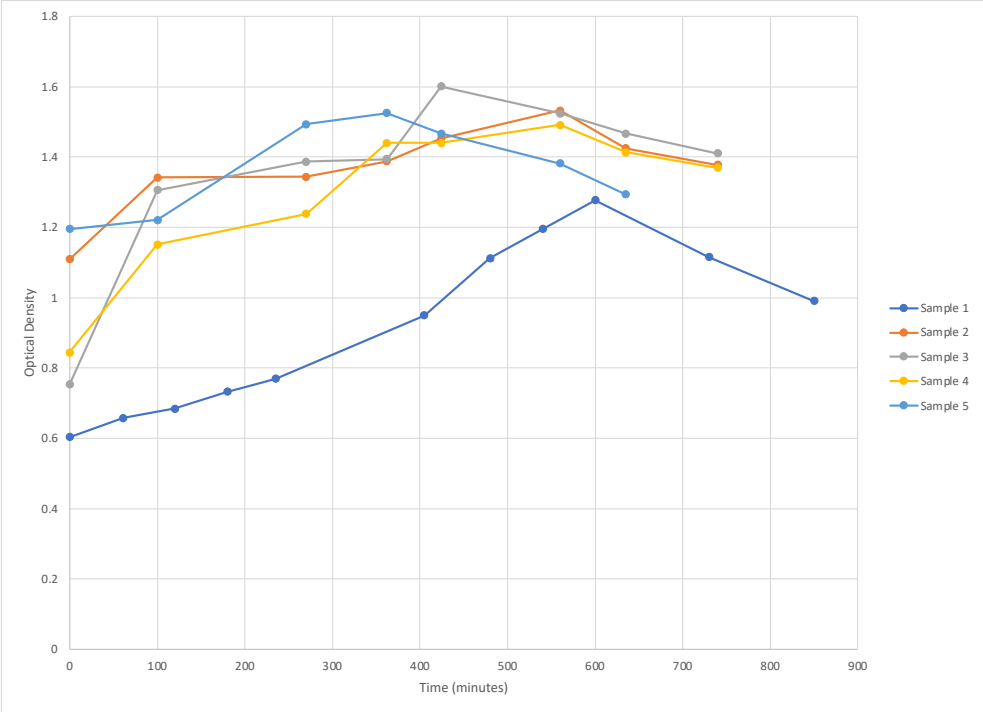

Figure 1. Growth Curve of Bacteria from Rotten Spinach Slime.

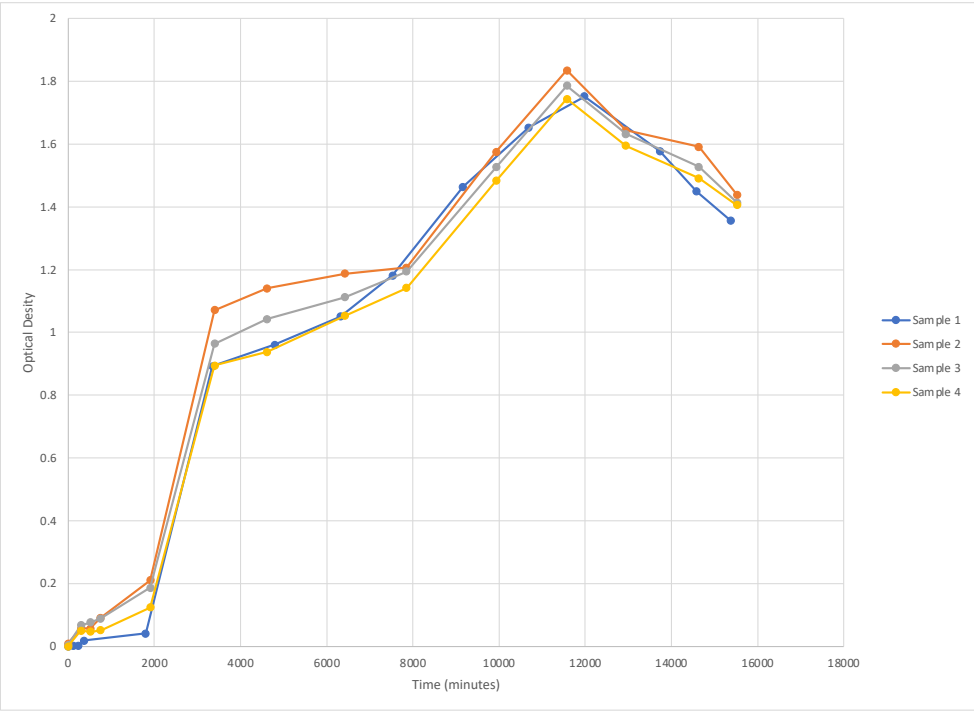

Figure 2. Growth Curve of Bacterial *Erwinia.*

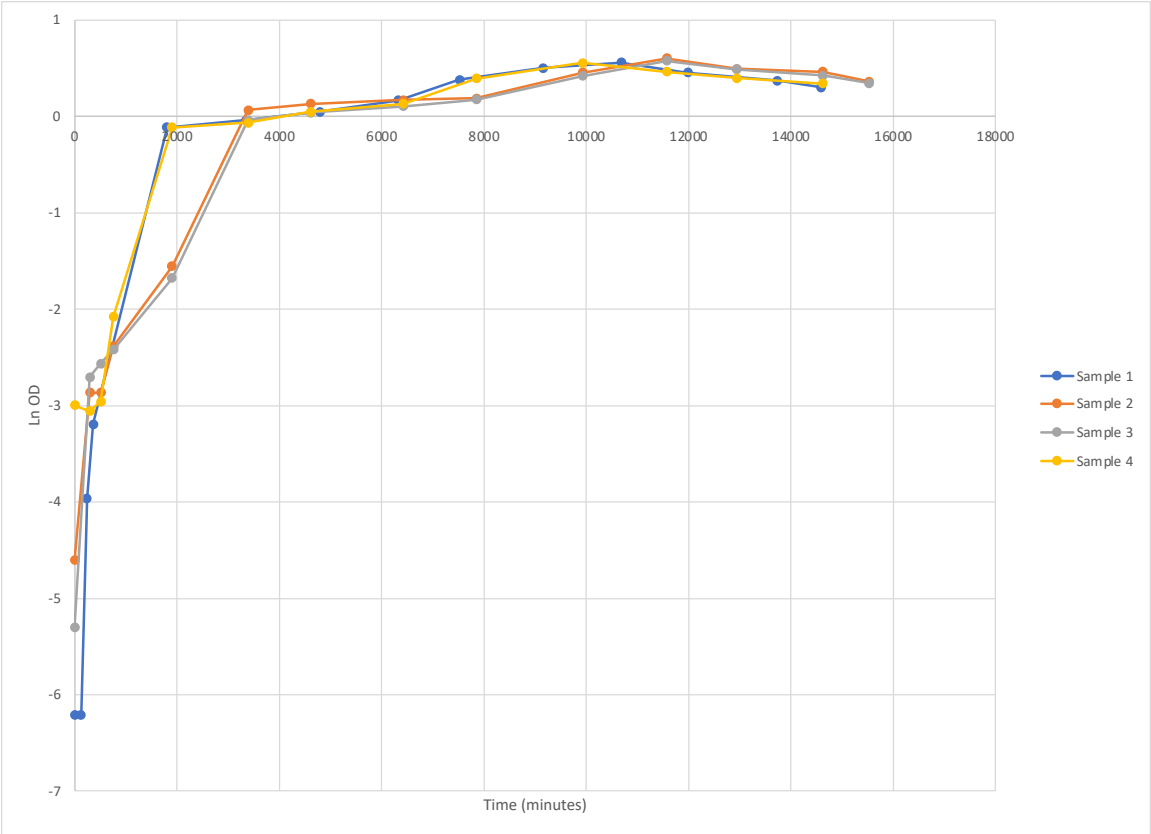

Figure 3. Growth curve of *Erwinia* Represented as ln OD versus Time (minutes).

Table 1. Contact Angles, electron-donor and electron acceptor parameters of the Lewis acid-base, and Lifshitz-van der Waals components of surface tension of *Erwinia* in units of mJ/m^2.

θ Water	θ Ethylene Glycol	θ Alpha Bromonaphthalene	γ_s^{LW} (mJ/m^2)	γ_s^+ (mJ/m^2)	γ_s^- (mJ/m^2)
26.45	26.51	50.70	29.62	0.59	61.78
26.45	26.51	51.60	29.17	0.64	61.90
26.45	26.51	51.64	29.15	0.64	61.90
26.45	26.51	52.02	28.96	0.66	61.95

26.45	29.34	50.70	29.62	0.45	63.39
26.45	29.34	51.60	29.17	0.49	63.50
26.45	29.34	51.64	29.15	0.49	63.51
26.45	29.34	52.02	28.96	0.51	63.56
26.45	33.54	50.70	29.62	0.25	66.09
26.45	33.54	51.60	29.17	0.28	66.21
26.45	33.54	51.64	29.15	0.28	66.21
26.45	33.54	52.02	28.96	0.30	66.26
26.94	26.51	50.70	29.62	0.60	61.24
26.94	26.51	51.60	29.17	0.65	61.35
26.94	26.51	51.64	29.15	0.65	61.36
26.94	26.51	52.02	28.96	0.68	61.41
26.94	29.34	50.70	29.62	0.46	62.84
26.94	29.34	51.60	29.17	0.50	62.95
26.94	29.34	51.64	29.15	0.50	62.96
26.94	29.34	52.02	28.96	0.52	63.01
26.94	33.54	50.70	29.62	0.26	65.53
26.94	33.54	51.60	29.17	0.29	65.64
26.94	33.54	51.64	29.15	0.29	65.65
26.94	33.54	52.02	28.96	0.31	65.70
27.21	26.51	50.70	29.62	0.61	60.94
27.21	26.51	51.60	29.17	0.66	61.05
27.21	26.51	51.64	29.15	0.66	61.06

27.21	26.51	52.02	28.96	0.68	61.10
27.21	29.34	50.70	29.62	0.46	62.54
27.21	29.34	51.60	29.17	0.50	62.65
27.21	29.34	51.64	29.15	0.51	62.65
27.21	29.34	52.02	28.96	0.52	62.70
27.21	33.54	50.70	29.62	0.26	65.22
27.21	33.54	51.60	29.17	0.29	65.33
27.21	33.54	51.64	29.15	0.30	65.34
27.21	33.54	52.02	28.96	0.31	65.39
Avg:			29.23	0.47	63.39
St. dev:			0.24	0.15	1.81

Table 3. High p-values with no significant difference observed (95% CI).

TiO_2 Concentrations	P-value
0 & 0.05 g/L TiO2	0.127
0 & 0.1 g/L TiO2	0.220
0 & 0.5 g/L TiO2	0.192
0.05 & 0.1g/L TiO2	0.292
0.05 & 0.5 g/L TiO2	0.342
0.1 & 0.5 g/L TiO2	0.450

Table 4. Low p-values with significant difference observed (95% CI).

TiO2 Concentrations	p-values

0 & 10.5 g/L TiO2	1.80E-07
0 & 16.8 g/L TiO2	8.42E-10
0 & 25.2 g/L TiO2	3.15E-11
0 & 31.5 g/L TiO2	1.95E-09
0.05 & 10.5 g/L TiO2	2.60E-03
0.05 & 16.8 g/L TiO2	4.65E-05
0.05 & 25.2 g/L TiO2	5.30E-05
0.05 & 31.5 g/L TiO2	2.68E-04
0.1 & 10.5 g/L TiO2	4.66E-03
0.1 & 16.8 g/L TiO2	4.57E-05
0.1 & 25.2 g/L TiO2	2.55E-04
0.1 & 31.5 g/L TiO2	1.85E-04
0.5 & 10.5 g/L TiO2	2.91E-03
0.5 & 16.8 g/L TiO2	1.56E-04
0.5 & 25.2 g/L TiO2	1.17E-04
0.5 & 31.5 g/L TiO2	8.38E-05
10.5 & 16.8 g/L TiO2	4.29E-05
10.5 & 25.2 g/L TiO2	3.27E-05
10.5 & 31.5 g/L TiO2	6.14E-06
16.8 & 25.2 g/L TiO2	4.36E-02
16.8 & 31.5 g/L TiO2	3.57E-04
25.2 & 31.5 g/L TiO2	3.98E-04